THE SMC RESULTS ON POLARIZED MUON-NUCLEON DEEP INELASTIC SCATTERING

I. A. SAVIN

Joint Institute for Nuclear Research, Joliot Curie str. 6, Dubna, 141980 Russia

E-mail: Igor.Savin@cern.ch

On behalf of the Spin Muon Collaboration (SMC)

The final SMC results on spin asymmetries A_1 and spin dependent structure functions g_1 of the proton and deuteron in the kinematic range $0.0008 < x < 0.7$ and $0.2 < Q^2 < 100$ GeV^2 are presented, together with the results of a next-to-leading order QCD analysis of the presently available data on g_1. The SMC data on asymmetries A_2 and structure functions g_2 and on semi-inclusive asymmetries $A^{+(-)}$ are briefly discussed as well.

1 Introduction

As it is well known, the inclusive Deep Inelastic Scattering (DIS) of polarized leptons on polarized nucleons

$$\vec{l} + \vec{N} \to l' + X, \tag{1}$$

is a reaction probing the nucleon spin structure. A theoretical double differential cross section of this reaction, $\sigma \equiv \mathrm{d}^2\sigma/\mathrm{d}x\mathrm{d}Q^2$, is calculated following the rules of the one-photon exchange Feynman diagram. It is expressed in terms of kinematic variables x and Q^2 and four structure functions two of which, $F_2(x,Q^2)$ and $R(x,Q^2)$, characterize the structure of unpolarized nucleons and two others, $g_1(x,Q^2)$ and $g_2(x,Q^2)$, represent the structure of polarized nucleons. The kinematic variables x and Q^2 in laboratory system are determined via the energies of incident and scattered leptons, E and E', respectively, and lepton scattering angle Θ : $Q^2 = 4EE'sin^2\Theta/2$, $x = Q^2/2M\nu$, $\nu = E - E'$, M is a nucleon mass. Variables E, E' and Θ are usually known for each event.

The phenomenology of DIS can be found in SMC publications (see the list) and references therein. As is shown there (see [11]), the spin dependent structure functions g_1^{p}, g_1^{d} and g_2^{p}, g_2^{d} of the proton and deuteron are expressed via experimentally measured cross section asymmetries $A_\parallel^{p,d}$ and $A_\perp^{p,d}$:

$$A_\parallel^{p,d} = \frac{\sigma_{\uparrow\downarrow}^{p,d} - \sigma_{\uparrow\uparrow}^{p,d}}{\sigma_{\uparrow\downarrow}^{p,d} + \sigma_{\uparrow\uparrow}^{p,d}}, \qquad A_\perp^{p,d} = \frac{\sigma_{\uparrow\rightarrow}^{p,d} - \sigma_{\uparrow\leftarrow}^{p,d}}{\sigma_{\uparrow\rightarrow}^{p,d} + \sigma_{\uparrow\leftarrow}^{p,d}}. \tag{2}$$

The asymmetry $A_{\parallel}^{p,d}$ ($A_{\perp}^{p,d}$) is measured with longitudinally polarized beam and longitudinally (transversely) polarized targets. In the one-photon exchange approximation they are related to the virtual photon asymmetries A_1 and A_2 and structure functions g_1 and g_2. To the first approximation

$$A_{\parallel}^{\mathrm{p,d}} \simeq D A_1^{\mathrm{p,d}}, \qquad\qquad A_{\perp}^{\mathrm{p,d}} \simeq d A_2^{\mathrm{p,d}}, \tag{3}$$

and

$$g_1^{\mathrm{p,d}} \simeq \frac{F_2^{\mathrm{p,d}}}{2x(1+R)} \cdot \frac{A_{\parallel}^{\mathrm{p,d}}}{D}, \qquad\qquad g_2^{\mathrm{p,d}} \simeq \frac{F_2^{\mathrm{p,d}}}{2x(1+R)} \cdot \frac{A_{\perp}^{\mathrm{p,d}}}{d}, \tag{4}$$

where D and d are virtual photon depolarization factors.

The structure function g_1 is of special interest to spin physics because in the Quark Parton Model (QPM) of the nucleon it can be interpreted as a difference of two probabilities, $q_i^{\uparrow}(x)$ and $q_i^{\downarrow}(x)$, averaged over the quark flavor charges:

$$g_1(x) = \sum_{i=1}^{n_f} e_i^2 [q_i^{\uparrow}(x) - q_i^{\downarrow}(x)] \equiv \sum_{i=1}^{n_f} e_i^2 \Delta q_i^{\uparrow\downarrow}(x). \tag{5}$$

Here $q_i^{\uparrow}(x)$ ($q_i^{\downarrow}(x)$) is the probability that in a longitudinally polarized nucleon quark i has a fraction x of the nucleon momentum and a spin aligned along (opposite to) the nucleon spin. To some extend, $g_1(x)$ characterizes a partial contribution of quarks to the nucleon spin.

The g_1 is also interesting for measurements aiming to test the famous Bjorken and Ellis-Jaffe sum rules. These sum rules involve the first moments of the structure function g_1, Γ_1 :

$$\Gamma_1^{p,d,n} = \int_0^1 g_1^{p,d,n}(x)\mathrm{d}x. \tag{6}$$

In QPM the Γ_1 represents a total contribution of active quark flavors to the nucleon spin.

The Bjorken sum rule for $\Gamma_1^{\mathrm{p}} - \Gamma_1^{\mathrm{n}}$ has been derived for the first time about 30 years ago in the asymptotic limit $Q^2 \to \infty$ using the quark current algebra and assuming standard quark charge assignments and isospin symmetry for quark distributions in nucleons :

$$\Gamma_1^{\mathrm{p}} - \Gamma_1^{\mathrm{n}} = \int_0^1 [g_1^p(x) - g_1^n(x)]\mathrm{d}x = \frac{1}{6}\left|\frac{g_A}{g_V}\right|, \tag{7}$$

where g_A (g_V) is the axial (vector) coupling constant of weak interactions. Now the Bjorken sum rule is derived in QCD. The Bjorken sum rule is independent of nucleon spin structure details and due to that is of the fundamental importance for the present understanding of elementary particles.

The Ellis-Jaffe sum rules for $\Gamma_1^{\rm p}$ and $\Gamma_1^{\rm n}$ have been derived initially using the same assumptions as for the Bjorken sum rule and additionally assuming the SU(3) symmetry in decays of the octet baryons and zero net polarization for strange sea quarks in nucleons :

$$\Gamma_1^{p(n)} = \int_0^1 g_1^{p,n}(x)\mathrm{d}x = +(-)\frac{1}{12}(F+D) + \frac{5}{36}(3F-D), \qquad (8)$$

where F and D are SU(3) couplings describing the β-decays of the baryon octet members. In QCD the Ellis-Jaffe sum rules are the subject of corrections.

The first measurement of the $g_1^p(x)$ has been performed by SLAC experiments E80 and E130 and published in 1980. The kinematic range of these measurements was x=0.1 – 0.7. Nothing unexpected has been seen either for $A_1^p(x)$ or for $g_1^p(x)$. Surprises came later, when in 1988 the European Muon Collaboration (EMC) at CERN has repeated the measurements of $g_1^p(x)$ in the extended x range from 0.01 to 0.7 and found that Γ_1^p is less than the Ellis-Jaffe prediction by about three standard deviations. From the measured Γ_1^p the EMC has found that quarks contribute little to the proton spin and strange quark sea is probably polarized negatively. The EMC results originated the so called spin crisis which became the subject of many experimental and theoretical works. New experiments have been suggested in 1989: SMC at CERN, SLAC E142 and E143, HERMES at DESY and later on SLAC E154 and E155.

The SMC experiment has been approved to start data taking in 1991. The main features of the experiment can be summarized as follows :
- longitudinally polarized muon beam at 100 and 200 GeV;
- high resolution spectrometer to measure parameters of scattered muons;
- two polarimeters to measure the polarization of the beam [2,20];
- the world largest polarized target with longitudinally or transversely polarized protons or deuterons [4,15-19].

The goals of the SMC were :

- to check the SLAC/EMC measurements on g_1^p with improved accuracy;
- to obtain new data on g_1^d and, as a consequence, on g_1^n ;
- to measure spin dependent structure function $g_2^{p,d}$ for the first time;
- to test the Bjorken sum rule for the first time.

SMC was taking the data during 150 days annually from 1991 to 1996 with various targets. Each year the collected data were analyzed (see [1,3,5-14]).

2 Spin dependent asymmetries $A_1^{p,d}$ and structure functions $g_1^{p,d}$ of the proton and deuteron

The SMC has calculated the asymmetries A_1 and structure functions g_1 from asymmetries $A_\parallel$ using the simplified expressions (3) and (4). Possible errors connected with this simplification are included in systematic uncertainties.

The experimentally measured asymmetry, $A_\parallel^{meas}$, is determined via counting rate asymmetries corresponding to the opposite settings of the target polarizations. To obtain the physics asymmetry $A_\parallel$ from $A_\parallel^{meas}$ one needs to apply corrections connected with finite target, P_T, and beam, P_B, polarizations as well as corrections connected with the dilution factor f':

$$A_\parallel^{meas} = f' P_B |P_T| A_\parallel . \tag{9}$$

The dilution factor f' depends on the fraction of polarized nucleons inside the target material, f, and on a ratio of one-photon exchange and total cross sections contributing to the counting rates. This ratio depends on the data selection procedure. For the final data on $A_1^{p,d}$ SMC has used two different methods of event selection. The first one corresponds to the inclusive events when only the scattered muon originating from the target is recognized regardless of other particles detected by the spectrometer for the particular event. The second method, additionally to the scattered muon, requires at least one hadron originating from the same vertex. The dilution factor $f'_{INC}(x)$ strongly depends on x and varies from about 0.05 to 0.2 in the SMC kinematic range while $f'_{HAD}(x)$ is almost constant in the same range. Combining the two methods one can gain in statistical accuracy for $A_\parallel$. Estimations have shown [13] that the optimal accuracy of data is obtained when for $x \leq 0.02$ the events are selected by the hadron method and for $x > 0.02$ - by the inclusive one.

The final SMC results on $A_1^{p,d}$ and $g_1^{p,d}$ are calculated using :
- the updated value of the beam polarization $P_B = -0.795 \pm 0.019$ [a];
- the reprocessed 1993 proton data with improvements which resulted in the statistic gain of about 10%;
- the new fits on $F_2^{p,d}$ including recently published NMC data.

Fig.1 shows the final SMC results on A_1 for the proton and deuteron compared to other data. In the low x-range, down to x=0.0008, the SMC data are unique. Each point in Fig.1 is given at the Q^2 value which is the average value for the particular x bin. In Fig.2 the data on A_1 are presented in x, Q^2-bins. No Q^2-dependence of A_1 is seen within the errors from these plots. The fit of the data by the constant for each x bin is shown by the dashed line.

[a] see the contribution of K.Medved in these Proceedings.

The final SMC data on $g_1^{p,d}(x)$ are presented in Fig.3. The lowest-x point is shown for the first time. It is calculated using three lowest x points in A_1 at x=0.0008-0.003 with Q^2 >0.2 GeV^2. This point is very important for understanding the low-x-behaviour of $g_1(x)$. Without it one can think that $g_1^p(x)$ is an increasing function of x. For the deuteron SMC has observed for the first time negative values of $g_1^d(x)$ at x <0.05.

The first moments of the $g_1^{p,d}(x)$ have been calculated using the data at Q^2 >1 GeV^2 and x=0.003–0.7. Each (x, Q^2) point was corrected to the common Q_0^2 using the expression

$$g_1(x,Q_0^2) = g_1(x,Q^2) + [g_1^{fit}(x,Q_0^2) - g_1^{fit}(x,Q^2)] \tag{10}$$

where g_1^{fit} is the NLO QCD fit result. At $Q_0^2 = 10\,\mathrm{GeV}^2$

$$\int_{0.003}^{0.7} g_1^{\mathrm{p}}(x,Q_0^2)dx = 0.131 \pm 0.005 \pm 0.006 \pm 0.004, \tag{11}$$

$$\int_{0.003}^{0.7} g_1^{\mathrm{d}}(x,Q_0^2)dx = 0.037 \pm 0.006 \pm 0.003 \pm 0.003. \tag{12}$$

Compared to previously published values [9-11] the central values in Eqs. (11) and (12) are changed by a few per cents mainly due to the updated value of the beam polarization. The contributions to the integrals from unmeasured regions are calculated from the parametrizations of parton distributions obtained from the QCD analysis (see Section 3). The final values of the moments differ from the Ellis-Jaffe predictions by several standard deviations:

	SMC	ELLIS-JAFFE	
$\Gamma_1^p(Q_0^2) =$	$0.120 \pm 0.005 \pm 0.006 \pm 0.014,$	$0.176(4),$	(13)
$\Gamma_1^d(Q_0^2) =$	$0.019 \pm 0.006 \pm 0.003 \pm 0.013,$	$0.068(4).$	(14)

Note, that the largest contributions to the errors come from theoretical uncertainties which have been underestimated in earlier publications.
Knowing the g_1^{p} and g_1^{d}, one can calculate a non-singlet structure function :

$$g_1^{\mathrm{NS}}(x,Q^2) = g_1^{\mathrm{p}} - g_1^{\mathrm{n}} = 2\left(g_1^{\mathrm{p}}(x,Q^2) - \frac{g_1^{\mathrm{d}}(x,Q^2)}{1-\frac{3}{2}\omega_D}\right), \tag{15}$$

where $\omega_D = 0.05 \pm 0.01$ is a probability for deuteron to be in a D-state.
This g_1^{NS} is interesting from several points of view :
- $g_1^{\mathrm{NS}}(x)$ is expected to have x-behaviour similar to that of $F_1^{\mathrm{NS}} = F_1^{\mathrm{p}} - F_1^{\mathrm{n}}$;

- Q^2-evolution of $g_1^{\rm NS}$ is determined by the evolution of non-singlet quark distributions only and does not involve gluons;
- the first moment of $g_1^{\rm NS}$ is the genuine Bjorken sum rule. It could be tested this way which is different from the generally used one.

For the $g_1^{\rm NS}$ and $F_1^{\rm NS}$ comparison (Fig.4), the latter is calculated using the F_2^d/F_2^p data of NMC, SMC fit of the world data on F_2 [13] and NMC/SLAC fit on R ($F_1 = F_2/2x(1+R)$). As is seen from this figure, the shapes of $g_1^{\rm NS}(x)$ and $F_1^{\rm NS}(x)$ are similar.

The Q^2-evolution of $g_1^{\rm NS}(x,Q^2)$ was studied by three different methods. All three methods gave the consistent values of $g_1^{\rm NS}(x,Q_0^2)$ at $Q_0^2 = 10$ GeV^2 . The evolved values of $g_1^{\rm NS}$ were used for calculations of the first moment :

$$\Gamma_1^{NS}(Q_0^2) = \int_0^1 g_1^{\rm NS}(x,Q_0^2)dx = 0.198 \pm 0.023 \tag{16}$$

to be compared with theoretical prediction 0.186±0.003 at $Q_0^2 = 10$ GeV^2 . This alternative way to test the Bjorken sum rule has some advantages due to smaller theoretical uncertainties.

3 The NLO QCD analysis of the SMC and world data on $g_1^{p,n,d}$

The final SMC and available world data on $g_1^{p,n,d}(x,Q^2)$ have been recently analysed [14] by the SMC in the most complete form.

In QCD the $g_1(x,t)$ is related to polarized parton (quark and gluon) distributions by an expression [11,14] :

$$\begin{aligned} g_1(x,t) = \tfrac{1}{2}\langle e^2\rangle \int_x^1 \frac{{\rm d}y}{y}\Big[& C_{\rm S}^q(\tfrac{x}{y},\alpha_s(t))\Delta\Sigma(y,t) \\ & + 2n_f C^g(\tfrac{x}{y},\alpha_s(t))\Delta g(y,t) + C_{\rm NS}^q(\tfrac{x}{y},\alpha_s(t))\Delta q_{\rm NS}(y,t)\Big], \end{aligned} \tag{17}$$

where $t = \ln(Q^2/\Lambda^2)$, Λ is the QCD scale parameter, $\langle e^2\rangle$ is the average squared quark charge, n_f is a number of active flavors, $\Delta\Sigma$ and $\Delta q_{\rm NS}$ are the singlet and non-singlet polarized quark distributions, Δg is the polarized gluon distribution, $C_{S,NS}^q(\alpha_s(t))$ and $C^g(\alpha_s(t))$ are the quark and gluon coefficient functions. The x- and Q^2 dependence of polarized parton distributions is given by the Dokshitser, Gribov, Lipatov, Altarelli, Parisi (DGLAP) evolution equations two of which, for $\Delta\Sigma$ and Δg, are coupled and third, for Δq_{NS}, is decoupled from Δg.

The DGLAP equations include also splitting functions defining probabilities for a given parton to emit the secondary parton. The polarized coefficient and splitting functions are calculated in QCD.

At the Next-to-Leading Order (NLO) in $\alpha_s(t)$ the splitting and coefficient functions depend on the QCD renormalizations and factorization schemes which are related to each other by known transformations. Two schemes are widely used, the first one is so called $\overline{\mathrm{MS}}$ scheme and the second is Adler-Bardin or AB scheme. In the $\overline{\mathrm{MS}}$ scheme the first moment of the gluon coefficient function C^g is equal to zero, i.e. gluons do not contribute to Γ_1. In the AB scheme gluons contribute to Γ_1 explicitly.

The SMC method of the QCD analysis of the $g_1(x, Q^2)$ is as follows.

The parton distributions defining the g_1 are searched for in a functional form taking into account the low- and high- x behaviour of structure functions at the initial Q_i^2 :

$$\Delta f(x, Q_i^2) = N(\alpha_f, \beta_f, a_f) \ \cdot \eta_f \ x^{\alpha_f}(1-x)^{\beta_f}(1 + a_f \ x), \tag{18}$$

where Δf denotes $\Delta\Sigma$, Δq_{NS} or Δg and $N(\alpha, \beta, a)$ is fixed by the normalization

$$N(\alpha, \beta, a) \int_0^1 x^\alpha (1-x)^\beta (1 + ax) dx = 1. \tag{19}$$

The initial parton distributions are evolved from Q_i^2 to Q^2 of the data points using DGLAP equations. The χ^2 is determined

$$\chi^2 = \sum_{i=1}^{n} \frac{\left[g_1^{\mathrm{calc}}(x, Q^2) - g_1^{\mathrm{data}}(x, Q^2)\right]^2}{(\delta_{\mathrm{stat}} g_1^{\mathrm{data}}(x, Q^2))^2}, \tag{20}$$

where g_1^{calc} are evolved values and δ_{stat} are the statistical errors of the data points. (The systematic errors are highly correlated from point to point and evaluated in a separate study, see [11,14]). Then the χ^2 is minimized by varying the coefficients η_f, α_f, β_f and a_f of the initial parton distributions to get the best fit to the data at the initial $Q_i^2 = 1$ GeV^2. To test the stability of the result, Q_i^2 was set to 10 GeV^2. No difference in the fit results was observed but precision of parameters was poorer.

To normalize the NS distributions, the parameters $\eta_{NS}^{p,n}$ were fixed using the neutron and hyperon β-decay constants and SU(3) flavor symmetry :

F/D = 0.575±0.016 and $|g_A/g_V|$ = F+D =1.2601±0.0025 .

This normalizations implies the Bjorken sum rule conservation. For the tests of this sum rule the constant $|g_A/g_V|$ was taken as free parameter.

Usually the strong interaction constant was fixed at $\alpha_s(M_z^2) = 0.118 \pm 0.003$ except for the special test to see if α_s, being considered as a free parameter, would be consistent within the errors with that obtained from the QCD analysis of unpolarized data. This special fit has given $\alpha_s(M_z^2) = 0.121 \pm 0.002 \pm 0.006$ in agreement with the standard value.

Two QCD programs are used: Program 1 developed by R.Ball et al. and working in moment space and Program 2 developed by SMC and working in (x, Q^2) space. The Program 2 is much faster and requires much less computer time. Final results which were obtained by the two programs for g_1 and parton distributions turned out to be identical.

In order to be consistent with other papers, the final results presented below are obtained with the Program 1. This Programs has the $\overline{\mathrm{MS}}$ and AB versions. The best fit parameters of the parton distributions obtained by each version are given in Table 1. There is a good agreement between the parameters in both schemes in the non-singlet sector. For the gluons the results are not in perfect agreement but consistent within quoted errors. For the singlet sector the results, as expected, are quite different. These features are illustrated in Fig.5. Note, that $\Delta q_{NS}^{p,n}$ are almost identical in the both schemes, $\Delta\Sigma$'s differ very much in the low x (unmeasured) regions and Δg is larger and shifted to the lower x in the AB scheme. But in the range of the data the best fits $g_1^{p,d,n}(x)$ obtained in $\overline{\mathrm{MS}}$ and AB schemes differ very little. This is also expected because the physics quantities should not depend on the factorization and normalization schemes.

Table 1: Comparison of the best fit results for the polarized parton distributions obtained by the NLO QCD Program 1 in the $\overline{\mathrm{MS}}$ and AB schemes

		$\overline{\mathrm{MS}}$	AB
SINGLET	η_{S}	$0.19^{+0.04}_{-0.05}$	$0.38^{+0.03}_{-0.03}$
	α_{S}	$-0.48^{+0.11}_{-0.10}$	$1.20^{+0.29}_{-0.27}$
	β_{S}	$3.29^{+0.40}_{-0.37}$	$4.08^{+0.63}_{-0.58}$
	a_{S}	$-13.8^{+1.3}_{-1.5}$	(0.0)
GLUON	η_g	$0.25^{+0.29}_{-0.22}$	$0.99^{+1.17}_{-0.31}$
	α_g	$0.33^{+2.05}_{-1.05}$	$-0.70^{+0.23}_{-0.20}$
	β_g	(4.0)	(4.0)
NON-SINGLET	$\alpha_{\mathrm{NS}}^{\mathrm{p}}$	$-0.19^{+0.09}_{-0.08}$	$-0.15^{+0.09}_{-0.08}$
	$\beta_{\mathrm{NS}}^{\mathrm{p}}$	$1.35^{+0.23}_{-0.21}$	$1.42^{+0.23}_{-0.22}$
	$\alpha_{\mathrm{NS}}^{\mathrm{n}}$	$0.06^{+0.14}_{-0.13}$	$0.01^{+0.13}_{-0.12}$
	$\beta_{\mathrm{NS}}^{\mathrm{n}}$	$2.59^{+0.52}_{-0.48}$	$2.48^{+0.51}_{-0.46}$
	χ^2/ndf	122.9/123	126.3/124

To preserve the consistency with previous SMC publications, the final results of the QCD analysis are presented in the AB scheme.

The NLO QCD fits to the world data on $g_1^p(x,Q_0^2)$, $g_1^d(x,Q_0^2)$, $g_1^n(x,Q_0^2)$ and $g_1^{NS}(x,Q_0^2)$ at $Q_0^2 = 5$ GeV^2 performed by SMC in AB scheme using the Program 1 are presented in Figs.6-9, respectively. The data points are shown with statistical errors only. The estimations of experimental systematic and theoretical uncertainties are given separately by vertically and horizontally hatched bands. Note the negative values of $g_1^p(x)$ predicted by present QCD analysis for $x \leq 10^{-3}$.

The QCD fits are used for calculations of first moments of the $g_1^{p,d,n}(x,Q_0^2)$. The results are given in Table 2. Note, that dominating errors come from uncertainties of low- x contributions.

Table 2: $\Gamma_1^{p,d,n}(Q_0^2)$ for the present world data

NUCLEON	$\Gamma_1(Q_0^2)$, $Q_0^2 = 5$ GeV^2
PROTON	$0.121 \pm 0.003 \pm 0.005 \pm 0.017$
DEUTERON	$0.021 \pm 0.004 \pm 0.003 \pm 0.016$
NEUTRON	$-0.075 \pm 0.007 \pm 0.005 \pm 0.019$

With the chosen normalization (19) of the parton distribution functions (PDF) (18) the parameters $\eta_{\rm g}$, $\eta_{\rm NS}$ and $\eta_{\rm s}$ are equal to the first moments of the gluon, non-singlet and singlet quark distributions at initial Q_i^2 and represent the contributions of the corresponding partons to the nucleon spin. The value of $\eta_{\rm g}(Q_i^2)$ at $Q_i^2 = 1$ GeV^2 obtained in the AB scheme (Table 1) has large statistical errors. Systematic errors estimated separately are also large:

$$\eta_{\rm g}(Q_i^2 = 1GeV^2) = 0.99^{+1.17+0.42+1.43}_{-0.31-0.22-0.45} \tag{21}$$

So, very little one can say about the gluon contribution to the spin of nucleon from the present data on g_1.

The singlet axial current matrix element a_0, representing the total quark contributions to the spin of the nucleon can be calculated from the QCD analysis in the two schemes at the initial Q_i^2. With the chosen normalization of PDF in $\overline{\rm MS}$ scheme $a_0(Q_i^2)_{\overline{\rm MS}}$ coincide with $\eta_s(Q_i^2)_{\overline{\rm MS}}$ while in the AB scheme the gluon contribution must be subtracted :

$$a_0(Q_i^2)_{AB} = \eta_{sAB} - n_f \frac{\alpha_s(Q^2)}{2\pi} \eta_g(Q_i^2)_{AB}. \tag{22}$$

Because the a_0 is a physics quantity, results should be scheme independent. It was found that in AB scheme at $Q_0^2 = 1$ GeV^2

$a_0 = 0.23 \pm 0.07(\mathrm{stat.}) \pm 0.19(\mathrm{syst.})$

while at the same Q_0^2 in the $\overline{\mathrm{MS}}$ scheme one gets

$a_0 = 0.19 \pm 0.05(\mathrm{stat.}) \pm 0.04(\mathrm{syst.})$,

i.e. the results are compatible.

From the global QCD fits of the world data, as well as from the QCD fits restricted to the non-singlet sector one can calculate $\Gamma_1^{\mathrm{p}} - \Gamma_1^{\mathrm{n}}$ and test the Bjorken sum rule. The SMC data alone have shown (see Section 2) that this rule is confirmed. The same conclusion can be drawn from the world data. At $Q_0^2 = 5$ GeV^2 :

	WORLD DATA	THEORY
$\Gamma_1^{\mathrm{p}} - \Gamma_1^{\mathrm{n}}$	$0.174^{+0.024}_{-0.012}$	0.181 ± 0.003

The integral under the solid line in Fig.9 with the total uncertainty which is shown by a hatched band represents the Γ_1^{NS}. Only the SMC and E143 data are used because for these calculations one needs to have the proton and deuteron data obtained by the same apparatus exactly at the same (x, Q^2) bins. The SMC and E143 data on Γ_1^{NS} confirm the Bjorken sum rule within 15% of its value at $Q_0^2 = 5$ GeV^2.

4 Spin dependent asymmetries $A_2^{p,d}$ and structure functions $g_2^{p,d}$

The spin dependent structure function $g_2(x, Q^2)$ has no direct physics interpretation. It is of a pure phenomenological nature and appears due to interference in an absorption of transversely and longitudinally polarized virtual photons by nucleons.

Properties of g_2 have been established in QCD in terms of twist-2, g_2^{WW} and twist-3, $\overline{g_2}$, contributions :

$g_2(x, Q^2) = g_2^{WW}(x, Q^2) + \overline{g_2}(x, Q^2)$.

The twist-2 contribution to g_2^{WW} can be calculated via the g_1. The $\overline{g_2}$ is predicted to be small.

There are Burkhardt-Cottinghem, Efremov-Leader-Teryaev and QCD sum rules involving g_2. These sum rules have not been fully tested yet due to the difficulty to estimate g_2 in the unmeasured region at low x.

Experimentally A_2 and g_2 are measured from the asymmetries $A_\perp$. The asymmetry A_2 and g_2 are bounded by the positive limit $|A_2| \leq \sqrt{R}$.

The data on asymmetries $A_2^{p,d}$ have been obtained by the SMC for the first time [6,9] and found to be much smaller than the positivity limit. They are consistent with zero in the range of measurements.

5 Semi-inclusive asymmetries

Asymmetries $A^{+(-)}$ in spin dependent cross sections for the production of positive (negative) hadrons in DIS reactions

$$\vec{\mu} + \vec{N} \to \mu + X + h^{\pm}, \tag{23}$$

are defined as

$$A^{+(-)} = \frac{\sigma_{\uparrow\downarrow}^{+(-)} - \sigma_{\uparrow\uparrow}^{+(-)}}{\sigma_{\uparrow\downarrow}^{+(-)} + \sigma_{\uparrow\uparrow}^{+(-)}} \tag{24}$$

where σ's are differential cross sections for a particular orientation of the lepton and nucleon spins. Similar to the inclusive asymmetries $A_{\parallel}$, the asymmetries $A^{+(-)}$ are related to the virtual photon asymmetry $A_1^{+(-)}$ [8,12].

The asymmetries $A_{1p}^{+(-)}$ and $A_{1d}^{+(-)}$ for the longitudinally polarized proton and deuteron are calculated [12] from about $5 \cdot 10^6$ h^+ and $4 \cdot 10^6$ h^- in the kinematic region x=0.003-0.7, $< Q^2 >$=10 GeV^2 and W>3 GeV. In QPM these asymmetries can be interpreted in terms of polarized quark distributions Δq and $\Delta \bar{q}$ and fragmentation functions D_q^h and $D_{\bar{q}}^h$. For example,

$$A_{1p}^{+(-)}(x,Q^2) = \frac{\sum_{q,h} e_q^2 \left[\Delta q(x,Q^2)\, D_q^h(Q^2) + \Delta\bar{q}(x,Q^2)\, D_{\bar{q}}^h(Q^2)\right]}{\sum_{q,h} e_q^2 \left[q(x,Q^2)\, D_q^h(Q^2) + \bar{q}(x,Q^2)\, D_{\bar{q}}^h(Q^2)\right]}. \tag{25}$$

One can show that from six measured asymmetries - A_{1p}, $A_{1p}^{+(-)}$, A_{1d}, $A_{1d}^{+(-)}$ - one can determine three distributions - of the polarized valence quarks and non-strange sea - Δu_v, Δd_v and $\Delta\bar{q}$. As it is shown in [12], $\Delta u_v(x)$ is positive and increases with x, $\Delta d_v(x)$ is negative and relatively flat in x and $\Delta\bar{q}(x)$ is consistent with zero. The average relative polarization of the valence quarks $|\Delta q_v/q_v|$ is about 50%.

The first moments of the polarized quark distributions are found to be:
$\Delta u_v = 0.77 \pm 0.10 \pm 0.08$,
$\Delta d_v = -0.52 \pm 0.014 \pm 0.09$,
$\Delta\bar{q} = 0.01 \pm 0.04 \pm 0.03$.
These values are consistent with inclusive results [11].

6 Conclusion

1. The SMC has presented its final data on the spin dependent asymmetries $A_1^{p,d}$ and spin dependent structure functions $g_1^{p,d}$ measured in the widest kinematic range available in present fixed target experiments. The g_1^d has been measured by SMC for the first time.

2. The perturbative QCD analysis of the SMC and world data on g_1 has been performed in the most complete way and found to be consistent with the data.
3. The first moments of the $g_1^{p,d}$, $\Gamma_1^{p,d}(Q_0^2)$ are determined for the SMC and world data using the results of the QCD analysis for extrapolations of $g_1(x, Q_0^2)$ in the unmeasured regions. The uncertainties of the low x extrapolations give the major contribution to the overal uncertainties of $\Gamma_1^{p,d}(Q_0^2)$.
4. The Bjorken sum rule for $\Gamma_1^{\mathrm{p}} - \Gamma_1^{\mathrm{n}}$ is tested in different ways and confirmed within 10-15% of its theoretical value. The Ellis-Jaffe sum rules for the proton and deuteron are found to be violated by more than 3 standard deviations, even including the large theoretical uncertainties.
5. The singlet quark and non-singlet quark distribution functions and their first moments are determined from the QCD analysis reasonably well. The original EMC results are confirmed: quarks contribute little to the nucleon spin.
6. The polarized gluon distribution is poorly determined by all existing data on inclusive DIS and is to be determined from semi-inclusive reactions dominated by the photon-gluon processes (HERMES, COMPASS, RHIC-SPIN).
7. The spin dependent asymmetries $A_2^{p,d}(x)$ and structure functions $g_2^{p,d}(x)$ have been measured by the SMC for the first time and found to be consistent with zero in the range of measurements.
8. The semi-inclusive spin dependent asymmetries $A_{1p,d}^{+(-)}$ for the production of positive (negative) hadrons in DIS complement the results obtained from inclusive DIS.

List of SMC publications

1. "Measurement of the Spin-dependent Structure Function $g_1(x)$ of the Deuteron", *Phys. Lett.* B **302**, 533 (1993).
2. "Measurement of the Polarization of a High Energy Muon Beam", *Nucl. Instrum. Methods* A **343**, 363 (1994).
3. "Combined Analysis of World Data on Nucleon Spin Structure Functions", *Phys. Lett.* B **320**, 400 (1994).
4. "Measurement of the Deuteron Polarization in a Large Target", *Nucl. Instrum. Methods* A **349**, 334 (1994).
5. "Measurement of the Spin-dependent Structure Function $g_1(x)$ of the Proton", *Phys. Lett.* B **329**, 399 (1994).
6. "Spin Asymmetry in Muon-Proton Deep Inelastic Scattering on a Transversely-Polarized Target", *Phys. Lett.* B **336**, 125 (1994).
7. "A New Measurement of the Spin-dependent Structure Function $g_1(x)$ of the Deuteron", *Phys. Lett.* B **357**, 248 (1995).

8. "Polarization of Valence and Non-Strange Sea Quarks in the Nucleon from Semi-inclusive Spin Asymmetries", *Phys. Lett.* B **369**, 93 (1996).
9. "The Spin-Dependent Structure function $g_1(x)$ of the Deuteron from Polarized Deep-Inelastic Muon Scattering", *Phys. Lett.* B **396**, 338 (1997).
10. "The Spin-Dependent Structure Function $g_1(x)$ of the Proton from Polarized Deep-Inelastic Muon Scattering", *Phys. Lett.* B **412**, 414 (1997).
11. "Spin Structure of the Proton from Polarized Inclusive Deep-Inelastic Muon-proton Scattering", *Phys. Rev.* D **56**, 5330 (1997).
12. "Polarized Quark Distributions in the Nucleon from Semi-Inclusive Spin Asymmetries", *Phys. Lett.* B **420**, 180 (1998).
13. "Spin Asymmetries A_1 and Structure Functions g_1 of the Proton and the Deuteron from Polarized High Energy Muon Scattering", *Phys. Rev.* D **58**, 112.001 (1998).
14. "A Next-to-leading Order QCD Analysis of the Spin Structure Function g_1", *Phys. Rev.* D **58**, 112.002 (1998).
15. Proceedings of 7th International Workshop on Polarized Target Materials and Techniques, 1994, in *Nucl. Instrum. Methods* A. 356 (1995):
    "The SMC Polarized Target", pp. 47-52;
    "Topics in NMR Polarization Measurement", pp.62-73;
    "High Precision Measurement of the Polarization in a Large Target",pp.79-82;
    "Estimation of Non-linearity innerPolarization Measurement", pp.83-87;
    "The Modulation Effect on the Dynamic Polarization of Nuclear Spins", pp.99-101.
16. "Large Enhancement of Deuteron Polarization with Frequency Modulated Microwaves", *Nucl. Instrum. Methods* A **372**, 339 (1996).
17. "A Line-shape Analysis for Spin-1 NMR Signals", *Nucl. Instrum. Methods* A **398**, 109 (1997).
18. "Measurement of Proton and Nitrogen Polarization in Ammonia and a Test of Equal Spin Temperature" CERN–PPE/98–066, 1997, accepted for publication in *Nucl. Instrum. Methods* A.
19. "The Polarized Double Cell Target of the SMC", to be submitted to *Nucl. Instrum. Methods* A.
20. "Measurement of the SMC Muon Beam Polarization using the Asymmetry in the Elastic Scattering off Polarized Electrons", to be submitted to *Nucl. Instrum. Methods* A.

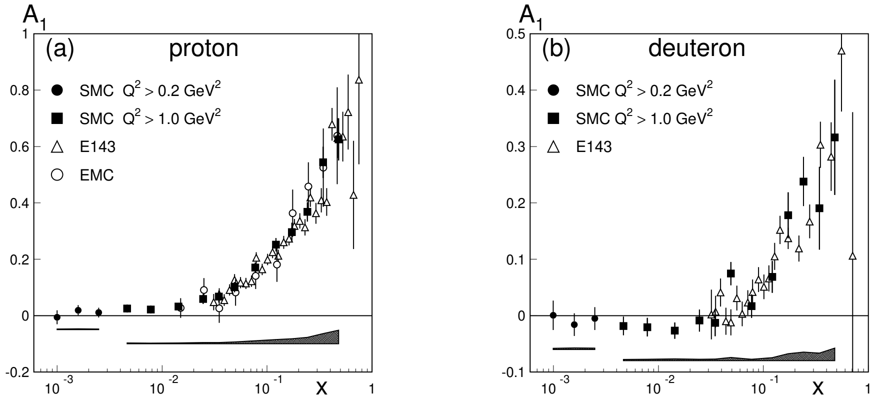

Figure 1: The final SMC results on A_1^p (a) and A_1^d (b) calculated from the optimal set of events requiring Q^2 >0.2 GeV^2 for three lowest x bins and $Q^2 > 1$ GeV^2 for other x bins. The data points are with statistical errors. The estimated systematic uncertainties are shown by hatched bands.

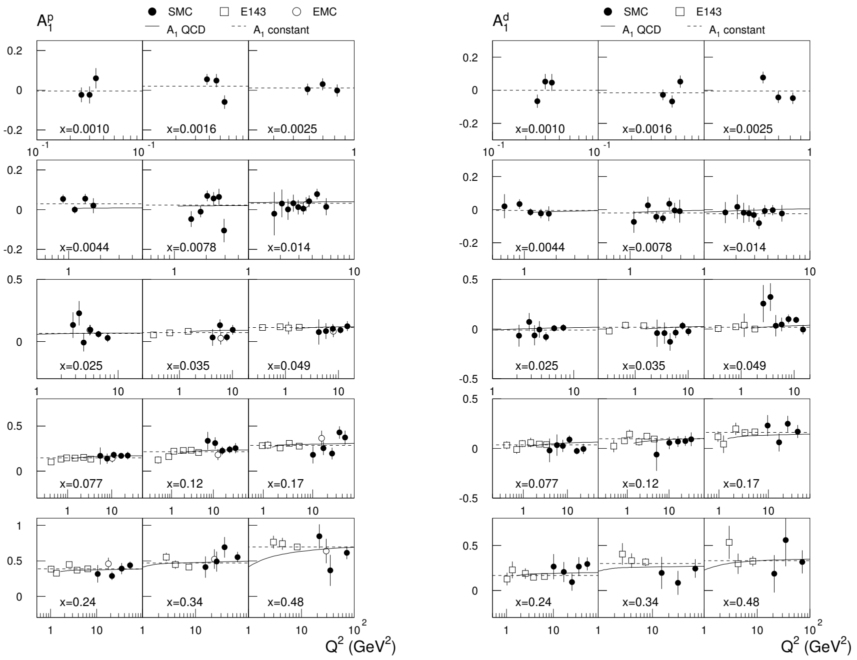

Figure 2: The final SMC results on $A_1^{\rm p}(x, Q^2)$ and $A_1^{\rm d}(x, Q^2)$ presented as a function of Q^2 for the x-bin the average value of which is given inside of each box. The solid lines show the results of the QCD fits described in Section 3.

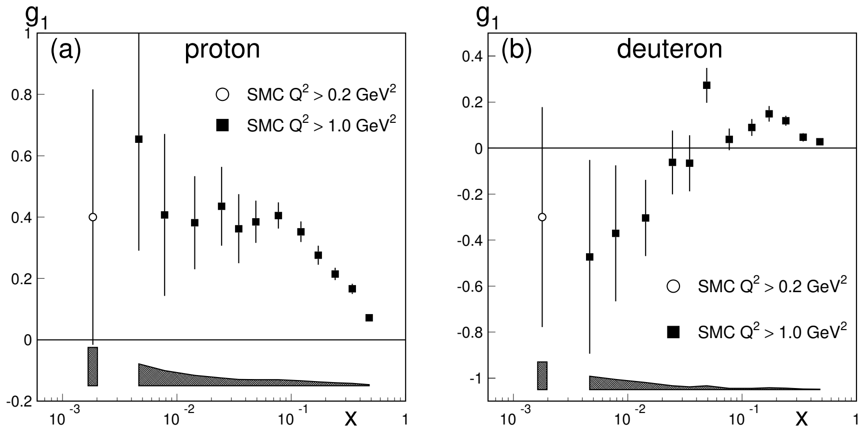

Figure 3: The final SMC results on $g_1^{\mathrm{p}}(x)$ (a) and $g_1^{\mathrm{d}}(x)$ (b).

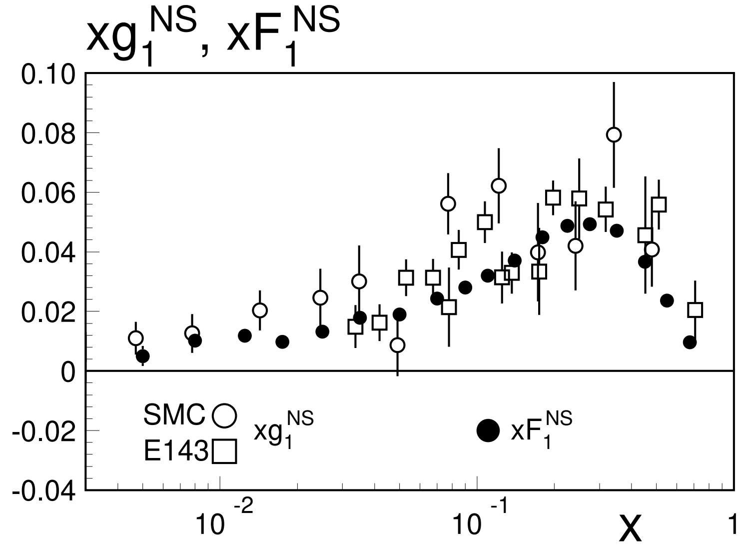

Figure 4: The non-singlet structure function $g_1^{\mathrm{NS}}(x)$ calculated from the SMC and SLAC E143 data on g_1^{p} and g_1^{d} and compared to F_1^{NS}.

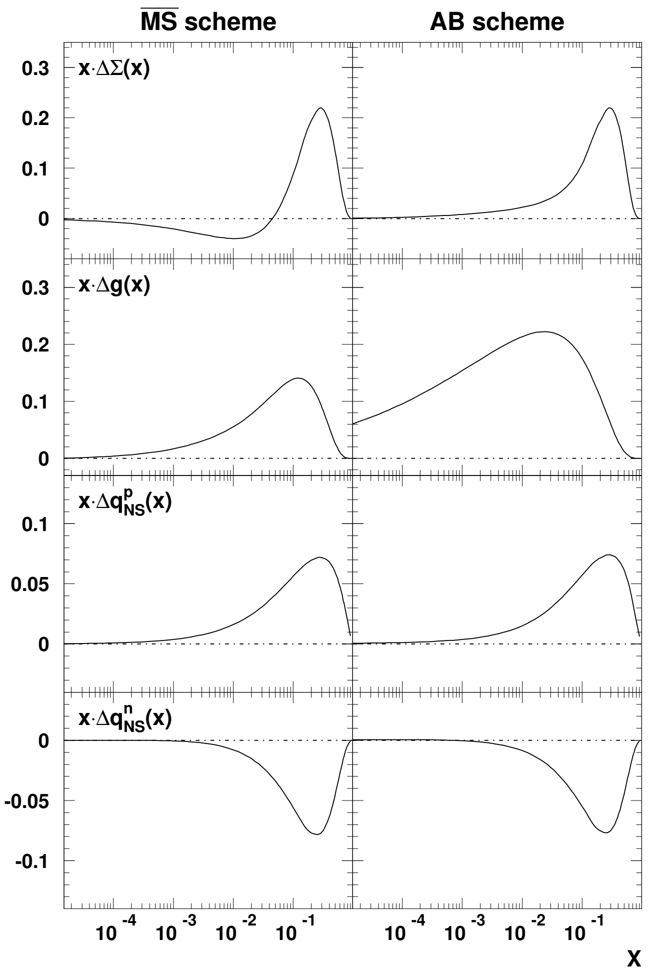

Figure 5: The parton distribution functions obtained from the QCD fits to the world data on $g_1(x, Q^2)$ using the $\overline{\text{MS}}$ and AB schemes.

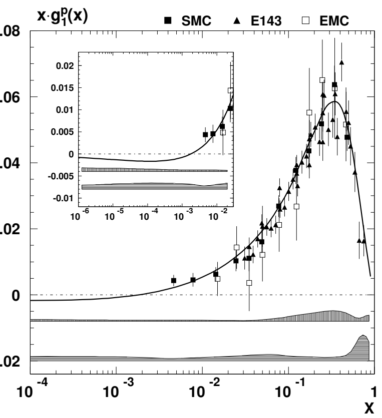

Figure 6: The results of QCD analysis on g_1^{p} compared to the data.

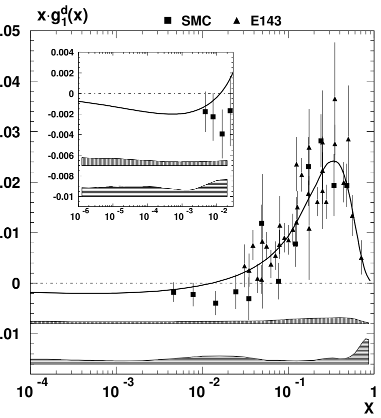

Figure 7: The same as in Fig.6 but for g_1^{d}.

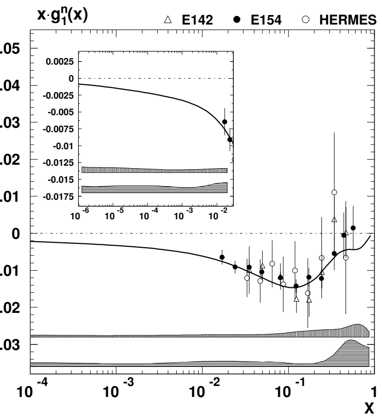

Figure 8: The same as in Fig.6 but for g_1^{n}.

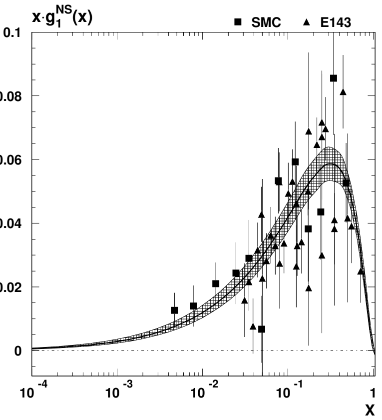

Figure 9: The same as in Fig.6 but for g_1^{NS}.